

Semiconducting chalcogenide buffer layer for oxide heteroepitaxy on Si(001)

D. A. Schmidt*

*Dept. of Physics & Center for Nanotechnology (CNT),
Univ. of Washington (UW), Seattle, WA 98195-1560*

Taisuke Ohta[†] and C.-Y. Lu

Dept. of Mat. Sci. and Engin. & CNT, UW, Seattle, WA 98195-2120

Aaron A. Bostwick[†] and Q. Yu[‡]

Dept. of Physics, UW, Seattle, WA 98195-1560

Eli Rotenberg

Advanced Light Source, Berkeley, CA 94720

F. S. Ohuchi

Dept. of Mat. Sci. and Eng. & CNT, UW, Seattle, WA 98195-2120

Marjorie A. Olmstead

Dept. of Physics & CNT, UW, Seattle, WA 98195-1560

(Dated: March 28, 2006)

We report controlled laminar growth of a crystalline transition metal oxide on Si(001) *without* SiO_x or silicide formation by utilizing the chalcogenide semiconductor gallium sesquiselenide (Ga₂Se₃) as a non-reactive buffer layer. Initial nucleation of both pure and Co-doped anatase (TiO₂) is along Ga₂Se₃ nanowire structures, coalescing to a flat, multidomain film within two molecular layers. Arsenic-terminated Si(001) (Si(001):As) is stable against pure O₂, but oxidizes when both Ti and O₂ are present. The Si–TiO₂ valence band offset using either buffer layer is about 2.8 eV, producing a staggered band alignment.

Integration of crystalline oxides with silicon is a critical component of myriad proposed applications, including spin-electronic (spintronic),^{1,2} ferroelectric and ferroic devices.³ Anatase-structure TiO₂, which is nearly lattice matched to Si, shows particular promise for Si-based nanoelectronics⁴ and, when doped with Co or Cr, spintronics.^{5,6} However, full integration of new crystalline-oxide-based functionalities into Si technology is currently impeded by spontaneous formation of amorphous oxides and/or silicides at the Si/oxide interface.

Sub-nanometer buffer layers can prevent interface reactions while preserving oxide functionality. Most notable among current buffers is a Sr-O interlayer for SrTiO₃ heteroepitaxy on Si(001),^{7,8} although substrate oxidation can occur during subsequent TiO₂ deposition.⁹ Ultrathin SiO₂ has been utilized for TiO₂ growth, resulting in an amorphous titanium silicate interface layer.¹⁰ An amorphous high band gap interlayer is acceptable for gate-insulator applications, but not for ferroelectric or ferromagnetic applications requiring crystalline oxides and/or non-scattering interfaces.

Here, we demonstrate a chalcogenide-based buffer layer, Ga₂Se₃/As, for laminar heteroepitaxy of both pure and cobalt-doped (5%) anatase (Co:TiO₂). Co:TiO₂ is known to be ferromagnetic at room temperature;^{5,6} Ga₂Se₃ has a band gap of 2.1 eV,^{11,12} between those of Si and TiO₂ (1.1 eV and 3.2 eV, respectively), and nearly the same lattice constant.¹³ Ga₂Se₃ forms a stable, epitaxial, non-reactive layer on Si(001):As.¹⁴ The intrinsic vacancy

structure of β -Ga₂Se₃, with one third of the cation sites vacant in a zinc-blende structure, also enables flexible strain relief. We observe neither oxide nor silicide formation at the buried Si interface, nor any buffer layer reactions; we also find a staggered band alignment, enabling electron transport from Si to TiO₂, but not vice versa. No evidence is found for the Co-rich surface clusters reported^{9,15,16} with other growth methods. These features are extremely promising for possible Si-based spintronic applications of Co:TiO₂. We also investigated Si(001):As as a buffer layer; it is stable in pure O₂, but allows oxidation of Si in the presence of Ti.

TiO₂ and Co:TiO₂ films and the As and Ga₂Se₃ buffer layers were deposited on clean *p*-type Si(001) ($\rho = 0.02\text{--}0.1 \Omega \cdot \text{cm}$) by molecular beam epitaxy and characterized *in situ* by scanning tunneling microscopy (STM), photoemission spectroscopy (PES), and x-ray absorption near-edge structure (XANES). Buffer layers were deposited as by Ohta et al.,¹⁴ first terminating the Si(001) surface with one monolayer of As and then adding ~ 0.8 nm Ga₂Se₃. Pure Ti or a Co:Ti alloy rod (95% Ti, 5% Co) was heated with an electron beam in an oxygen background ($P_{O_2} = 5 \times 10^{-5}$ torr) to deposit TiO₂ or Co:TiO₂ at either room or elevated (350–400°C) temperature. XANES measurements showed films grown at either room temperature (RT) or 350°C to have a Ti L-edge structure consistent with anatase standards grown on LaAlO₃(001), and inconsistent with rutile. Higher temperature deposition (500–600°C) results in growth of

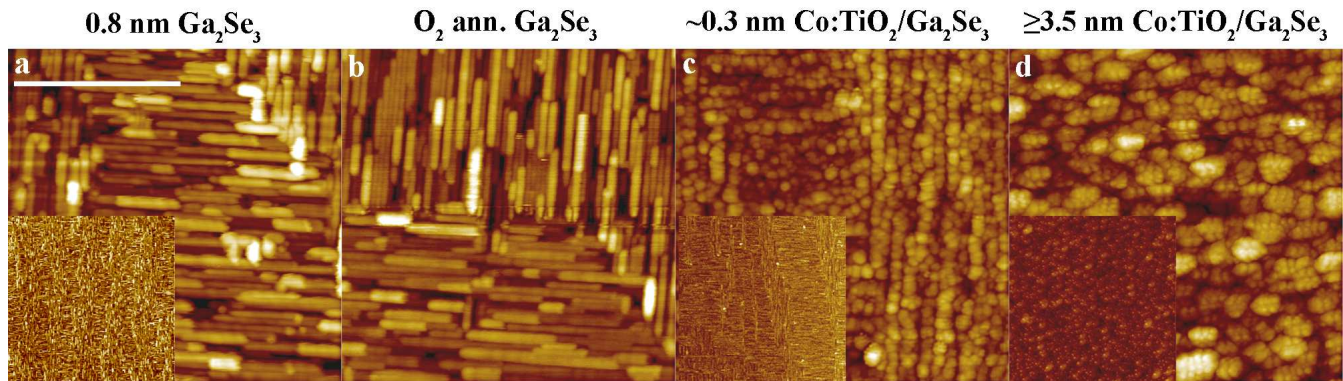


FIG. 1: **Surface morphology of buffer layers and oxide film.** (Color online) $100 \times 100 \text{ nm}^2$ STM images ($500 \times 500 \text{ nm}^2$ insets): (a) $\sim 0.8 \text{ nm Ga}_2\text{Se}_3$; (b) O_2 ($P_{\text{O}_2} \sim 5 \times 10^{-5} \text{ torr}$) annealed ($T_{\text{ann}} = 450^\circ\text{C}$) Ga_2Se_3 ; (c) $\sim 0.3 \text{ nm Co:TiO}_2$ film on $\sim 0.8 \text{ nm Ga}_2\text{Se}_3$; (d) $\geq 3.5 \text{ nm Co:TiO}_2$ film on $\sim 0.8 \text{ nm Ga}_2\text{Se}_3$. Scale bar in (a) is 50 nm. Nanoridges are in $[110]$ directions and differ in height by 0.27 nm. Image conditions: (a) 2.5 V, 0.07 nA, inset: -4.5V, 0.09 nA; (b) 2.8 V, 0.1 nA; (c) 2.8V, 0.09 nA, inset: 2.8V, 0.09 nA; (d) 2V, 0.12 nA, inset: 2.9V, 0.1 nA.

rutile nanocrystals; still higher destroys the buffer layer and oxidizes the substrate.¹⁷

The Ga_2Se_3 buffer layer self-assembles into oriented nanoridges, tens of nm long and 1-2 nm wide at their base [Fig. 1(a)], generated by ordered coalescence of intrinsic vacancies at the surface. The Ga-topped ridges have (111) Se facets forming the sides and change direction at each substrate step.^{14,18} This morphology is stable against oxidation in a partial pressure of $P_{\text{O}_2} = 5 \times 10^{-5} \text{ torr}$ at 450°C [compare Figs. 1(a) and (b)]. Photoemission spectroscopy shows no oxygen accumulation (within an experimental sensitivity of $\lesssim 2\%$ of a monolayer). The observed narrowing, smoothing and aligning of the nanoridge morphology also occurs during an equivalent anneal without O_2 ($P_{\text{tot}} \leq 1 \times 10^{-10} \text{ torr}$). The root-mean-square (rms) surface roughness over $1.0 \mu\text{m}^2$ is 0.24 nm, comparable to that of bare Si(001) (see Table I). On a smaller scale [Fig. 2(a), $30 \times 50 \text{ nm}^2$], six nanoridge levels (0.27 nm height difference) are exposed on what was originally two Si terraces.

RT deposition of about 1 molecular layer (ML) Co:TiO_2 on this $\text{Ga}_2\text{Se}_3/\text{As}$ buffer layer nucleates as 1 ML high clusters with centers spaced by 2-3 nm along the Ga_2Se_3 nanoridges [Fig. 1(c)]. The large-scale nanoridge morphology is unchanged (Fig. 1 insets). The first 1-2 ML have comparable roughness to the starting buffer layer (Table I). Deposition at 350°C [Fig. 2(c)] produces comparable morphologies, although the higher temperature (faster diffusion) growth leads to a larger spacing (3-4 nm) between the clusters. At coverages just below 1 ML, some underlying Ga_2Se_3 nanorods may be seen [*e.g.*, $x = 14-18 \text{ nm}$ in Fig. 2(f)-c], and sub-ML modulation is apparent on some larger surface islands.

Continued growth of Co:TiO_2 at either RT or 350°C results in laminar films without large surface clusters [inset, Fig. 1(d)]. At a thickness of $\sim 15-20 \text{ ML}$, the rms roughness of films grown at 350°C has increased by only $\sim 1/3 \text{ ML}$ over the starting value (Table I); the film exhibits

predominantly single ML height steps surrounding 5-10 nm diameter, kidney-bean shaped domains [Fig. 2(e)]. RT-deposited films are slightly rougher, exhibiting 7-10 nm diameter islands, 3-4 ML high [Figs. 2(d) and 1(d)].

Bright dots of apparent height 0.1 nm, spaced by $\sim 4-6$ surface unit cells, are seen in the positive tip bias, filled-state images of $T_{\text{dep}} = 350^\circ\text{C}$ Co:TiO_2 films [Fig. 2(e)]. Although we cannot rule out Co clustering, their spacing matches the expected distance between uniformly distributed Co atoms, which comprised 5% of the source metal. Similar bright spots, though with higher density and concentrated at step edges, were reported for STM of Co:TiO_2 films on SrTiO_3 ,¹⁹ where they were attributed to isolated Co atoms that remained after clusters dissolved upon annealing. In bulk Co:TiO_2 , Co^{2+} substitution for Ti^{4+} likely has an associated oxygen vacancy; a bright spot in occupied state images (presumably dominated by O $2p$ emission) indicates enhanced negative charge, consistent with an intact O lattice near a surface Co^{2+} impurity. The local morphology of pure TiO_2 films (not shown) is indistinguishable from Co:TiO_2 except for these bright dots.

Chemical reactions at the buried Si-buffer layer inter-

TABLE I: **Z-range RMS roughness (nm) as a function of preparation and scan size.** For anatase films, Co:TiO_2 values in roman, TiO_2 in *italics*; deposition at RT, with $T_{\text{dep}} = 350^\circ\text{C}$ in parentheses.

| Scan Range (μm^2) | Bare | | $\sim 0.8 \text{ nm Ga}_2\text{Se}_3$ | $\sim 0.3 \text{ nm Co:TiO}_2$ | $\geq 3.5 \text{ nm Co:TiO}_2$ |
|--------------------------------|---------|------------|---------------------------------------|--------------------------------|--------------------------------|
| | Si(001) | Si(001):As | | <i>TiO}_2</i> | <i>TiO}_2</i> |
| 1.0×1.0 | 0.26 | 0.14 | 0.24 | 0.21 | 0.32 |
| | | | | 0.27 (0.29) | 0.36 |
| 0.5×0.5 | 0.19 | 0.10 | 0.23 | <i>0.29 (0.28)</i> | <i>0.40 (0.34)</i> |
| | | | | 0.28 (0.24) | 0.35 |
| 0.1×0.1 | 0.06 | 0.07 | 0.29 | <i>0.28 (0.26)</i> | <i>0.43 (0.35)</i> |

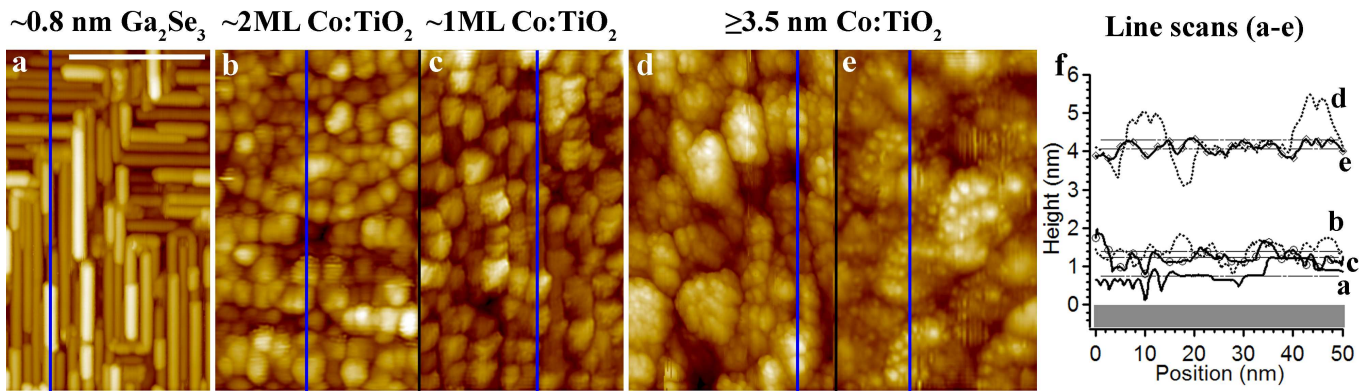


FIG. 2: **High resolution surface morphology of buffer layer and oxide films.** (Color online) $30 \times 50 \text{ nm}^2$ STM images of: (a) $\sim 0.8 \text{ nm Ga}_2\text{Se}_3$; (b-e) Co:TiO_2 films on $\sim 0.8 \text{ nm Ga}_2\text{Se}_3$: (b) $\sim 0.2 \text{ nm}$ (2 ML), $T_{dep} = \text{RT}$; (c) $\sim 0.08 \text{ nm}$ (1 ML), $T_{dep} = 350^\circ\text{C}$; (d) $\geq 3.5 \text{ nm}$ (20 ML), $T_{dep} = \text{RT}$; (e) $\geq 3.5 \text{ nm}$ (20 ML), $T_{dep} = 350^\circ\text{C}$; (f) cross-sectional line scans [110] (vertical lines) from (a-e). (a) solid line, (b) dotted line, (c) solid+circles, (d) dotted line, (e) solid+diamonds. Scale bar in (a) is 20 nm. Image conditions: (a) -5.4 V , 0.09 nA ; (b-c) 2.8 V , 0.09 nA ; (d) 1.8 V , 0.09 nA (e) 3.6 V , 0.1 nA .

face were investigated with photoemission spectroscopy (PES) at the Advanced Light Source in Berkeley, CA (Beamline 7.0.1) (Fig. 3). Both $\text{Si}(001):\text{As}$ and Ga_2Se_3 buffer layers are inert in partial pressures of O_2 ($P_{\text{O}_2} = 5 \times 10^{-5} \text{ torr}$) and $T_{\text{ann}} \leq 500^\circ\text{C}$. High resolution, surface-sensitive, core-level spectroscopy (Fig. 3) reveals no oxidized Si component for either Ga_2Se_3 or $\text{Si}(001):\text{As}$. In the presence of both Ti and O_2 , a significant oxidized Si $2p$ component is observed for $\text{Si}(001):\text{As}$ (peak at 102 eV in Fig. 3), indicating Ti catalyzes the Si–O reaction. The As $3d$ (not shown) also shows a reacted component upon TiO_2 deposition. TiO_2 growth on $\text{Ga}_2\text{Se}_3/\text{Si}(001):\text{As}$, however, shows no reacted substrate components. As the TiO_2 film grows thicker, the Si $2p$ peak neither shifts in energy nor shows any additional components; likewise the Ga $3d$, As $3d$, and Se $3d$ emission (not shown). All substrate peaks attenuate exponentially, as expected for a non-reactive, laminar deposition.¹⁷

We propose the TiO_2 nuclei react with the Se-terminated sides or valleys between the nanoridges. Ga–Ti interactions would lead to metallic states in PES, while Ga–O reactions would cause a new Ga $3d$ component; neither were observed. Interface Ti–Se interactions, on the other hand, may not have a clear PES signature. Se atoms with non-bonded lone pair orbitals can effectively “oxidize” the Ti adatoms and stabilize them at the surface for reaction with incident O_2 . No O adsorbs without Ti present. For $\text{Si}(001):\text{As}$, we suggest that Ti rests in the trenches between the As dimer rows, weakening the Si–As bonds to promote Si oxidation. The larger bond enthalpy of Si–O relative to Ti–O leads to preferential bonding to Si.

A key parameter for possible electronic device applications of TiO_2/Si is the band alignment. Fig. 3 shows valence band emission, highlighted with lines marking the band edges, using the known energy difference²⁰ between our measured Si $2p$ or Ti $3p$ emission and the respective

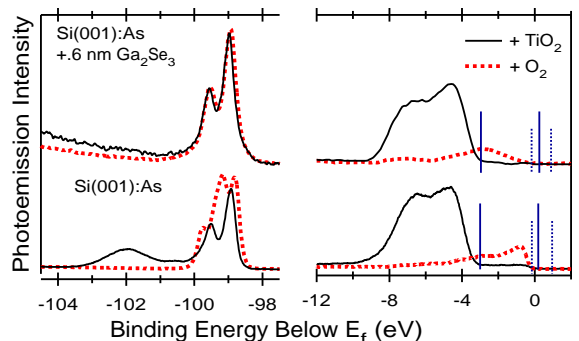


FIG. 3: **Chemical passivity of buffer layer.** (color online) Si $2p$ (left) and valence band (right) normal emission photoelectron spectra for $\text{Si}(001):\text{As}$ (bottom) and $\text{Si}(001):\text{As} + 0.6 \text{ nm Ga}_2\text{Se}_3$ (top) plus O_2 (dotted curve) or $\sim 0.5 \text{ nm TiO}_2$ film (solid curve). Photon energy, $h\nu = 160 \text{ eV}$. Si $2p$ peak intensities scaled to same area. Vertical lines show location of VBM and CBM for TiO_2 (solid) and Si (dotted) (see text).

VBM, and band gaps of 3.2 eV for anatase and 1.1 eV for Si. The valence band offset (VBO) is $2.77 \pm 0.1 \text{ eV}$ for the Ga_2Se_3 buffer layer and $2.86 \pm 0.1 \text{ eV}$ for As alone. These are well above the VBO values of $1.65\text{--}2.55 \text{ eV}$ for TiO_2 on a SiO_2 buffer layer,¹⁰ 1.93 eV for $\text{SrO}/\text{SrTiO}_2$ buffers,²⁰ and 2.0 eV predicted from alignment of charge neutrality levels.²¹ This indicates a significant interface dipole contribution from the As and Ga_2Se_3 buffer layers, possibly including As interdiffusion into the Ga_2Se_3 film. It should therefore be possible to shift this alignment through manipulation of interface dipoles in the Ga_2Se_3 film. Our measured VBO identifies a staggered band alignment, with the anatase CBM about 0.7 eV below of that of Si; this allows electron transport from Si to TiO_2 , but forms a barrier in the other direction.

In summary, we presented heteroepitaxy of laminar

TiO₂ and Co:TiO₂ on Si(001) without reactions at the buried silicon interface through use of Ga₂Se₃ as a buffer layer. The oxide nucleates between Ga₂Se₃ nanoridges, with further growth leading to laminar films with low surface roughness. No segregated particles are observed. We do not find successful oxide heteroepitaxy on As-terminated silicon. Finally, we find a staggered band alignment between the TiO₂ film and the Si substrate. We believe Ga₂Se₃ films may be extended for use as a buffer layer with other oxide heteroepitaxial systems.

This work was supported by NSF Grant ECS 0224138

and M. J. Murdock Charitable Trust. D. A. S. further acknowledges support from the UW-PNNL Joint Institute for Nanoscience and T. O. from the UW-CNT University Initiative Fund. Some data were obtained at the Advanced Light Source in Berkeley, CA (DOE Contract No. DE-AC03-76SF00098). The authors thank S. A. Chambers for fruitful discussions and for epitaxial anatase and rutile sample standards. Portions of this work were submitted by D. A. S. in partial fulfillment of the requirements for the Ph.D. at UW.

-
- * Present address: International Center for Young Scientists, NIMS, Tsukuba, Japan.
- † Present address: Advanced Light Source, Berkeley, CA 94720
- ‡ Present address: CNT, UW, Seattle, WA 98195-2140
- ¹ S. A. Wolf, D. D. Awschalom, R. A. Buhrman, J. M. Daughton, *Science* **294**, 1488 (2001).
 - ² D. D. Awschalom, M. B. Flatte, N. Samarth, *Scientific American* **286**, 66 (2002).
 - ³ J. B. Goodenough, *Rep. Prog. Phys.* **67**, 1915 (2004).
 - ⁴ S. A. Campbell, H.-S. Kim, D. C. Gilmer, B. He, T. Ma, and W. L. Gladfelter, *IBM J. Res. Develop.* **43**, 383 (1999).
 - ⁵ Y. Matsumoto, M. Murakami, M. Shono, T. Hasegawa, T. Fukumura, M. Kawasaki, P. Ahmet, T. Chikyow, S. Koshihara, and H. Koinuma, *Science* **291**, 854 (2001).
 - ⁶ S. A. Chambers, S. Thevuthasan, R. F. C. Farrow, R. F. Marks, J. U. Thiele, L. Folks, M. G. Samant, A. J. Kellock, N. Ruzycski, D. L. Ederer, and U. Diebold, *Appl. Phys. Lett.* **79**, 3467 (2001).
 - ⁷ R. A. McKee, F. J. Walker, M. F. Chisholm, *Phys. Rev. Lett.* **81**, 3014 (1998).
 - ⁸ R. A. McKee, F. J. Walker, M. B. Nardelli, W. A. Shelton, G. M. Stocks, *Science* **300**, 1726 (2003).
 - ⁹ T. C. Kaspar, T. Droubay, C. M. Wang, S. M. Heald, A. S. Lea, and S. A. Chambers, *J. Appl. Phys.* **97**, 073511 (2005).
 - ¹⁰ C. C. Fulton, G. Lucovsky, R. J. Nemanich, *Appl. Phys. Lett.* **84**, 580 (2004).
 - ¹¹ C.-S. Yoon, K.-H. Park, D.-T. Kim, T.-Y. Park, M.-S. Jin, S.-K. Oh, W.-T. Kim, *J. Phys. Chem.* **62**, 1131 (2001).
 - ¹² S. Morley, M. von-der-Emde, D. R. T. Zahn, V. Offermann, T. L. Ng, N. Maung, A. C. Wright, G. H. Fan, I. B. Poole, and J. O. Williams *J. Appl. Phys.* **79**, 3196 (1996).
 - ¹³ The unreconstructed (001) surface lattice parameters for β -Ga₂Se₃, Si and anatase TiO₂ are $a_s = 0.382$ nm, 0.383 nm and 0.379 nm, respectively. The (001) step heights are multiples of 0.274, 0.136 and 0.24 nm for Ga₂Se₃, Si and anatase, respectively.
 - ¹⁴ Taisuke Ohta, D. A. Schmidt, Shuang Meng, A. Klust, Q. Yu, M. A. Olmstead, and F. S. Ohuchi, *Phys. Rev. Lett.* **94**, 116102 (2005).
 - ¹⁵ S. A. Chambers, T. Droubay, C. M. Wang, A. S. Lea, R. F. C. Farrow, L. Folks, V. Deline, and S. Anders, *Appl. Phys. Lett.* **82**, 1257 (2003).
 - ¹⁶ J.-Y. Kim, J.-H. Park, B.-G. Park, H.-J. Noh, S.-J. Oh, J. S. Yang, D.-H. Kim, S. D. Bu, T.-W. Noh, H.-J. Lin, H.-H. Hsieh, and C. T. Chen, *Phys. Rev. Lett.* **90**, 017401 (2003).
 - ¹⁷ D. A. Schmidt, Ph.D. Thesis, Univ. of Washington (2005).
 - ¹⁸ T. Ohta, Ph.D. Thesis, Univ. of Washington (2004).
 - ¹⁹ J. S. Yang, D. H. Kim, S. D. Bu, T. W. Noh, S. H. Phark, Z. G. Khim, I. W. Lyo, and S.-J. Oh, *Appl. Phys. Lett.* **82**, 3080 (2003).
 - ²⁰ A. C. Tuan, T. C. Kaspar, T. Droubay, J. W. Rogers, Jr., and S. A. Chambers, *Appl. Phys. Lett.* **83**, 3734 (2003).
 - ²¹ J. Robertson, *J. Vac. Sci. Technol. B* **18**, 1785 (2000).